Estimation of low frequency part of the acoustic impedance from band-limited reflection data using first principles only

Animesh Mandal, Department of Earth Sciences, IIT Kanpur, India; and Santi Kumar Ghosh, Theoretical Modeling Group, CSIR-National Geophysical Research Institute, Hyderabad, India*

Email: animeshm@iitk.ac.in, santighosh@rediffmail.com

Keywords
Impedance reconstruction, Low-frequency, Field data, Singular Value Decomposition, Inversion

Summary
Estimation of the low frequency part of the acoustic impedance is an essential yet challenging tasks for quantitative interpretation from seismic data which is essentially band-limited in nature. Ghosh and Mandal (2016) had devised an effective solution using first principles only and demonstrated its efficacy through synthetic examples. Now in the present paper, we illustrate the method's success on real data, thus, corroborating the internal consistency of the basic approach. The present work also establishes that the effective reconstruction of broad and smooth impedance profile is possible from first principles and band-limited field data. The main features of this work is demonstrating the ability to reconstruct an approximate impedance profile without the aid of an initial model or statistical assumption on the reflectivity series. The approximate impedance profile can serve as reliable initial input for more refined inversion or geologic interpretation.

Introduction

Estimation of acoustic impedance is the ultimate goal of seismic data processing. Accurate reconstruction of this acoustic impedance helps to extract the detailed subsurface lithology. Such reconstruction assumes normally incident plane wave source, data free from multiples, and out of plane events etc., with correct relative amplitudes, and zero phase wavelet with flat amplitude spectrum. However, the band limitation of seismic reflection data leads to imperfect computation of the acoustic impedance. According to Ghosh (2000) the impulse response for reflection, $R(t)$ is proportional to the derivative (with respect to time) of the logarithm of acoustic impedance, t denoting the two-way travel time. Thus, for an imperfect, i.e., band-limited version of $R(t)$, the resulting reconstruction of the impedance function would also be imperfect and nonunique. A reasonable estimate of the impedance profile would, however, require a broadband estimate of $R(t)$ and would need to overcome the nonuniqueness employing either auxiliary information, often nonseismic or constraints characterizing the impedance model. Historically, the issue of nonuniqueness has been addressed in a variety of ways, e.g., with an initial model or by resorting to an assumption of certain criterion such as sparsity of the reflection coefficients etc. (Yilmaz, 2000). Therefore, the reconstruction of acoustic impedance from the band-limited seismic reflection data remains to be one of the major challenges to the geoscientists dealing with seismic exploration study.

Beginning from the restriction of band-limited reflection data, Ghosh and Mandal (2016) has devised a method for reconstructing broadband acoustic impedance using first principles (i.e., Zoeppritz's equations) only and without requiring any starting model or mathematical constraints. With the synthetic examples they have demonstrated the effectiveness of their method in reconstructing an approximate and smooth impedance profile by solving a set of linear equations through singular value decomposition (SVD). Thus, they have shown the feasibility of reconstructing low frequency (broad and smooth) part of acoustic impedance from band-limited synthetic data but they have not applied that approach in field data. In this work, we propose logical extensions of the earlier method (Ghosh and Mandal, 2016) and illustrate their success on real data, corroborating the internal consistency of the basic approach. Following the strategy of Ghosh and Mandal (2016), four bands are employed in order to arrive at consistent estimates of broad features of the impedance profile from field data. Nyquist criterion constrains the number of non-redundant sample points. Non uniqueness is addressed in part by limiting the number of layers to the number of sample points constrained by Nyquist criterion and in part by resorting to SVD method of solving the set of equations. The efficacy of the proposed method has been demonstrated with real seismic data where the acoustic impedance log is also available for verification.

Approximate broadband impedance reconstruction from field data

Theory and/or Method

The impulse response $R(t)$ of a stack of homogeneous and horizontal layered earth model (characterized by n reflection coefficients in the given time window) is given by (Oldenburg et al., 1983; Ghosh and Mandal, 2016)

$$R(t) = \sum_{k=1}^{n} r_k \delta(t - t_k) \quad (1)$$

where a typical reflection coefficient r_k occurs at $t = t_k$. Again, the seismic reflection data is conceived as the convolution of an embedded wavelet and the reflection coefficients (Robinson and Treitel, 1980). Thus, seismic data $d(t)$ can be represented as

$$w(t) * R(t) = d(t) \quad (2)$$

where $w(t)$ is the wavelet, $R(t)$ is the impulse response for a layered earth model, and '*' denotes convolution. Now convolving with the band-limited Heaviside function $H_b(t)$ (Ghosh, 2000; Ghosh and Mandal, 2016) on both side of equation (2), it can be written as

$$H_b(t) * w(t) * R(t) = H_b(t) * d(t). \quad (3)$$

The $H_b(t)$ will have a form of $\left(\frac{1}{\pi}\right)(\mathrm{Si}\, 2\pi f_H t - \mathrm{Si}\, 2\pi f_L t)$ [where, $\mathrm{Si}\, x = \int_0^x \left(\frac{\sin u}{u}\right) du$] where f_H and f_L are the effective upper and lower band limits that prevail in the data (Ghosh, 2000; Ghosh and Mandal, 2016). Now, denoting $W_I(t)$ for $H_b(t) * w(t)$, and $T(t)$ for $H_b(t) * d(t)$ the equation (3) can be represented as

$$W_I(t) * R(t) = T(t). \quad (4)$$

The equations (1) and (4) together lead to

$$\sum_{k=1}^{n} r_k W_I(t - t_k) = T(t) \quad (5)$$

The equation (5) contains n unknowns in the r_k s and n unknowns in the t_k s. The solution for the $2n$ unknowns are possible when one assumes that the t_k s are equispaced with uniform time interval designated as time-step resulted from every difference of $(t_{k+1} - t_k)$. Then, the equation (5) can be solved for the r_k s using the known values of the right side at all time points. In matrix form, the equation (5) can be rewritten as

$$\mathbf{Wr} = \mathbf{d}, \quad (6)$$

where $\mathbf{W}$ is a matrix whose k^{th} column consists of the sampled values of $W_I(t - t_k)$, $\mathbf{r}$ is a column vector $[r_1, r_2, \ldots, r_n]^{\mathrm{T}}$ corresponding, respectively, to times $t_1, t_2, \ldots, t_n$, and $\mathbf{d}$ is a column vector consisting of the sampled values of $T(t)$, for the pertinent time range. The equation (6) can now be solved for the unknown reflection coefficients by the method of singular value decomposition (SVD) as prescribed by Ghosh and Mandal (2016). Once the reflection coefficients are known, the impedance profile can be reconstructed from the known impedance at time $t = 0$, recursively using the formula

$$A_{k+1} = A_k \frac{1+r_k}{1-r_k}, \quad (7)$$

where A_k is the acoustic impedance of the k^{th} layer (Berteussen and Ursin, 1983).

Solution with SVD

According to a theorem in linear algebra (Press et al., 1992), any $m \times n$ matrix $\mathbf{W}$, whose number of rows m is greater than or equal to its number of columns n, can be decomposed as

$$\mathbf{W} = \mathbf{U\Sigma V}^{\mathrm{T}}, \quad (8)$$

where $\mathbf{U}$ is an $m \times n$ column-orthogonal matrix, $\mathbf{\Sigma}$ is an $n \times n$ diagonal matrix with nonnegative diagonal entries $\sigma_1, \sigma_2, \sigma_3, \ldots \sigma_n$ (known as the singular values of $\mathbf{W}$) ordered according to $\sigma_1 > \sigma_2 > \sigma_3 > \ldots > \sigma_n$, and $\mathbf{V}$ is an $n \times n$ orthogonal matrix. The formal least-squares solution of equation (6) turns out to be

$$\mathbf{r} = \mathbf{V\Sigma}^{-1}\mathbf{U}^{\mathrm{T}}\mathbf{d}, \quad (9)$$

where $\mathbf{\Sigma}^{-1}$ is an $n \times n$ diagonal matrix with diagonal elements $\sigma_1^{-1}, \sigma_2^{-1}, \sigma_3^{-1}, \ldots \sigma_n^{-1}$. Thus, it is obvious that the existence of very small singular values would tend to amplify the error of computation and results in unstable solution. Following the recommendation of Ghosh and Mandal (2016), we truncate the singular value series at a certain small singular value, designated as the terminal singular value (TSV) (suppose σ_m) and systematically enhance the value of TSV (keeping remaining $(m-1)$ values unchanged) according to the following three categories to achieve best possible solution for the impedance profile.

(a) First category: the TSV is kept unchanged.
(b) Second category: the TSV (σ_m) is replaced by its harmonic mean with the next higher singular value (i.e., with σ_{m-1}).
(c) Third category: the TSV is replaced by the next higher singular value (i.e., by σ_{m-1}).

For each category mean and standard deviation (SD) were calculated along with the impedance profile. SD represents a measure of the fluctuations of the profile. In moving across the choices from (a) to (b) and then to (c) the effective TSV successively increases. This progressively leads to the smoother reconstruction of the impedance profile. The truncation of the set of singular values and computation of the impedance profiles resulting from the above choices can be repeated gradually and systematically. Eventually a stage should come when the excursion across successive categories for the UTSV (suppose σ_k) do

not result in successively smoother solutions for the impedance profile. At this stage, the impedance mean and SD would become nearly stationary across the three categories. Thus, the solution for the impedance profile can be said to have achieved a saturation stage, i.e., solution become oversmooth. However, a less smooth solution would be more realistic and desirable. Accordingly, we would come back one step when the next smaller singular value (i.e., σ_{k+1}) was the UTSV and perform the reconstructions for four different bands to arrive at consistent estimates of the approximate impedance profile.

Tackling the reconstruction from field data

Above computational steps proceed along the line of Ghosh and Mandal (2016) which dealt only with synthetic traces contaminated by random noises. But real data contains two additional complications. First, the real data will contain a bulk time shift w.r.t. the synthetic trace (Veeken and Da Silva, 2004). This bulk shift originates as an artefact of the data acquisition and processing steps (Veeken and Da Silva, 2004). We must restore the real data to its correct temporal location by applying an adequate time shifts. Second, the synthetic data (Ghosh and Mandal, 2016) had the true amplitudes, whereas the real data contains only the relative amplitudes. The relative amplitude can be transformed to the true amplitude by knowing the true reflection coefficient at certain key reflectors. The latter effectively yields a scale factor connecting the true and relative amplitudes. We propose a novel approach to solve this problem. We assume that the impedance mean is known from the statistic of the impedance as measured in the well of the neighborhood. It turns out that this knowledge solves at onego the problem of knowing the scale factor and that of choosing the proper terminal singular value.

Results

The available acoustic impedance log, wavelet, Fourier spectrum of the wavelet, trace data, and the generated synthetic trace are shown in Figure 1a-1d. Based on the frequency limits of the wavelet spectrum (around 12 Hz and 83.33 Hz, Figure 1c), the present approach has been tested on a time-migrated field trace data for four frequency bands, namely, 12–31.25 Hz, 12–41.75 Hz, 12–62.5 Hz, and 12–83.33 Hz. The time lag between the field trace and synthetic trace was calculated by cross-correlating them (Figure 2a-2b). It was observed that the synthetic trace is delayed by 72 ms w.r.t. the field trace and accordingly last 72 ms of the field trace was deleted for reconstruction. For the same reason, the reconstructed impedance profile will have values after 72 ms when compared with the original log.

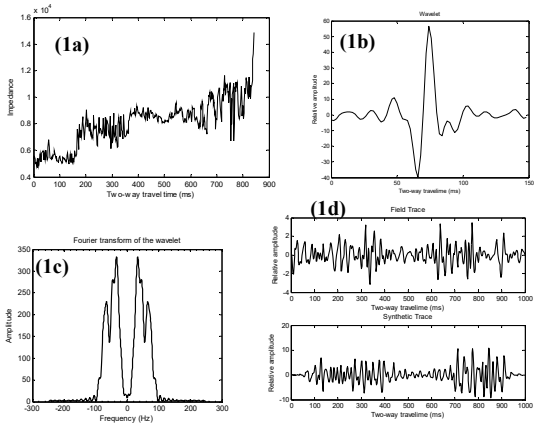

Figure 1: (a) Observed acoustic impedance log, (b) wavelet, (c) Fourier spectrum of the wavelet, (d) Field trace (upper panel) and Synthetic trace (lower panel).

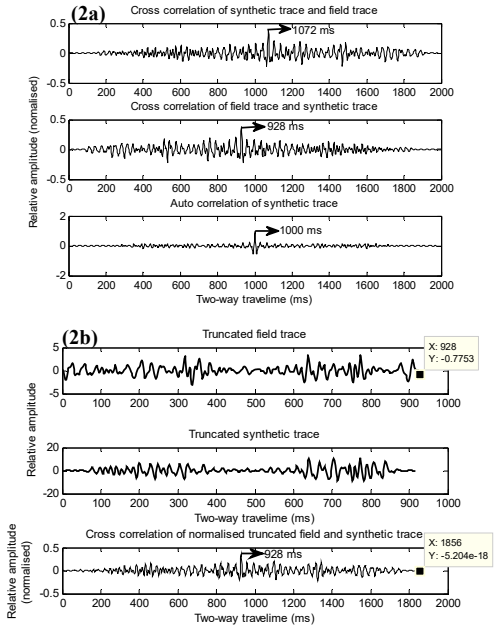

Figure 2: (a) Cross-correlation of synthetic and field trace (top panel), that of field and synthetic trace (middle panel), and auto-correlation of synthetic trace, (b) Truncated field trace (after removal of last 72 ms) (top panel), Truncated synthetic trace (middle panel), and cross-correlation of truncated field and truncated synthetic trace.

Now the reflection coefficients are estimated from the truncated field data for each of the above four frequency bands by solving the set of linear equations encapsulated in equation (6) by way of implementing equation (9). This is carried out according to the strategy of discarding small singular values as mentioned in the subsection *'Solution with SVD'*. Next, one obtains from the derived reflection coefficients an estimate of the impedance profile using the known value of the impedance at the initial time using equation (7) for each frequency band. To understand the quality of reconstruction, the mean misfit magnitude (MMM) (Ghosh and Mandal, 2016) of each reconstruction was calculated according to

$$\text{MMM}=\frac{1}{n}\left[\sum_{k=1}^{n}\left|\frac{(A_k-A_k')}{A_k}\right|\right], \qquad (10)$$

where A_1, A_2,….,A_k…..,A_n are the actual impedance values, and A_1', A_2',…,A_k',…..,A_n' are, respectively, their reconstructed versions.

Table 1 presents, for each band of frequencies, the results of trials with nine specific TSVs from three successive groups leading to three impedance means and SDs corresponding to the three impedance profiles from each group. The Figure 3a and 3b captures the essence of Table 1 and shows plots for normalized (dividing a given mean or SD value by its maximum over the corresponding frequency band) means and SDs across three groups consisting of nine values from each band. Evidently, the last group (with highest UTSV) in each band distinctly displays stationary behavior in impedance mean and standard deviation. Thus, next group (with lower UTSV) is expected to contain the best estimate of the impedance profile and we focus on that lower UTSV groups for which a consistent estimate of impedance across various bands is available. We impose the constraints that the trial impedance mean in a given band is close to the actual impedance mean (8246) of the log data, excluding initial 72 ms. Inspection over the four bands yield the following near-consistent estimates of the mean of the impedance profile: 8268 (12–31.25 Hz), 8140 (12–41.75 Hz), 8204 (12–62.5 Hz) and 8181(12–83.33 Hz) (Table 1). It is significant that these estimates and their mean of 8198 compare favorably with the actual impedance mean of 8246 of the log data.

The efficacy of the impedance reconstructions for the four bands are demonstrated by the overplots of the reconstructed impedance profiles over the original in Figure 4a–4d (upper panels). Broad highs and lows of the actual log are recovered satisfactorily in reconstructed impedance profile across all the four bands. In addition, the data used for reconstruction and the data that the reconstructed models would give rise to match remarkably well (Figure 4a–4d; lower panels). The MMM values for these reconstructions for the above four frequency bands (in the order of increasing upper band limit) are 0.145, 0.141, 0.145, and 0.141, respectively. Thus, the reconstructions are also good.

Table 1: Impedance mean and standard deviation computed for three categories of the TSV per group resulting from one UTSV ($\sigma_U = \sigma_k$) and two of its variants ($\sigma_H = [2\sigma_k\sigma_{k-1}/(\sigma_k + \sigma_{k-1})]$; and $\sigma_R = \sigma_{k-}$). The description includes three successive groups for each of the frequency bands (e.g., 12–31.25, 12–41.75, 12–62.5, and 12–83.33).

Frequency Band (Hz)	Time-step of t_k (ms)	Singular values (σ)		Progressive Category number across three groups	Mean of Reconstructed Impedance	Standard Deviation of reconstructed impedance
		Unmodified terminal singular value (UTSV) for a group	Terminal singular value (TSV) for a category			
12–31.25	16	8.24 (σ_{k+2})	σ_U = 8.24	1	7199	1215.2
			σ_H= 11.31	2	7712	1139.9
			σ_R= 18.04	3	8268	1079.9
		18.04 (σ_{k+1})	σ_U = 18.04	4	9313	1048.7
			σ_H= 23.92	5	8560	762.4
			σ_R = 35.49	6	7875	529.9
		35.49 (σ_k)	σ_U = 35.49	7	6646	249.6
			σ_H= 44.32	8	6576	238.3
			σ_R = 59.00	9	6508	228.7
12–41.75	12	9.93 (σ_{k+2})	σ_U = 9.93	1	7520	810.5
			σ_H= 13.65	2	7823	781.8
			σ_R = 21.83	3	8140	763.6
		21.83 (σ_{k+1})	σ_U = 21.83	4	8702	765.1
			σ_H= 28.81	5	8153	582.9
			σ_R = 42.36	6	7642	432.6
		42.36 (σ_k)	σ_U = 42.36	7	6669	248.6
			σ_H= 52.62	8	6581	232.2
			σ_R = 69.43	9	6494	218.2
12–62.5	8	12.22 (σ_{k+2})	σ_U = 12.22	1	7483	934
			σ_H= 16.75	2	7834	897.7
			σ_R = 26.63	3	8204	871.8
		26.63 (σ_{k+1})	σ_U = 26.63	4	8878	862.9
			σ_H= 35.06	5	8225	637.5
			σ_R= 51.29	6	7625	451.5
		51.29 (σ_k)	σ_U = 51.29	7	6484	217.9
			σ_H= 63.59	8	6417	208.4
			σ_R = 83.64	9	6352	200.3
12–83.33	6	13.94 (σ_{k+2})	σ_U = 13.94	1	7592	872.7
			σ_H= 19.09	2	7880	849.1
			σ_R = 30.28	3	8181	833.1
		30.28 (σ_{k+1})	σ_U = 30.28	4	8723	829.5
			σ_H= 31.49	5	8615	791.9
			σ_R = 32.80	6	8509	755.3
		32.80 (σ_k)	σ_U = 32.80	7	6343.4	208.9
			σ_H= 36.51	8	6363.1	208.6
			σ_R= 41.18	9	6342.8	208.3

The impedance profiles corresponding to the respective mean estimates can be treated as the reconstructed impedance profiles for the respective bands (Figure 4a–4d).

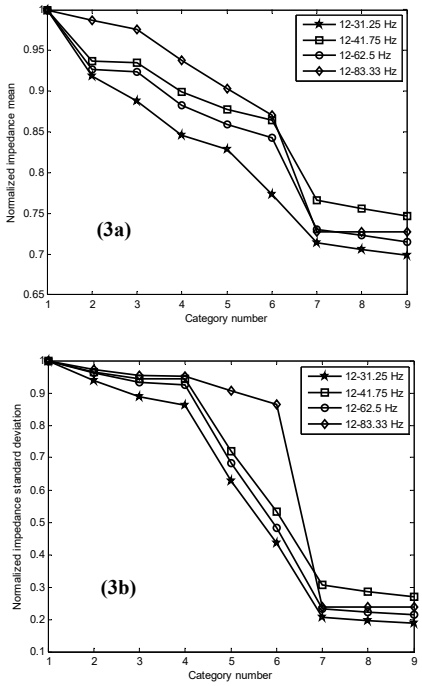

Figure 3: (a) normalized impedance mean vs category number and (b) normalized impedance SD vs category number. The category number corresponds to the number of progressively increasing TSVs shown for a particular band (see Table 1).

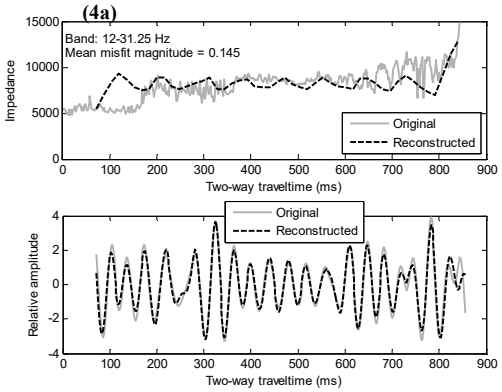

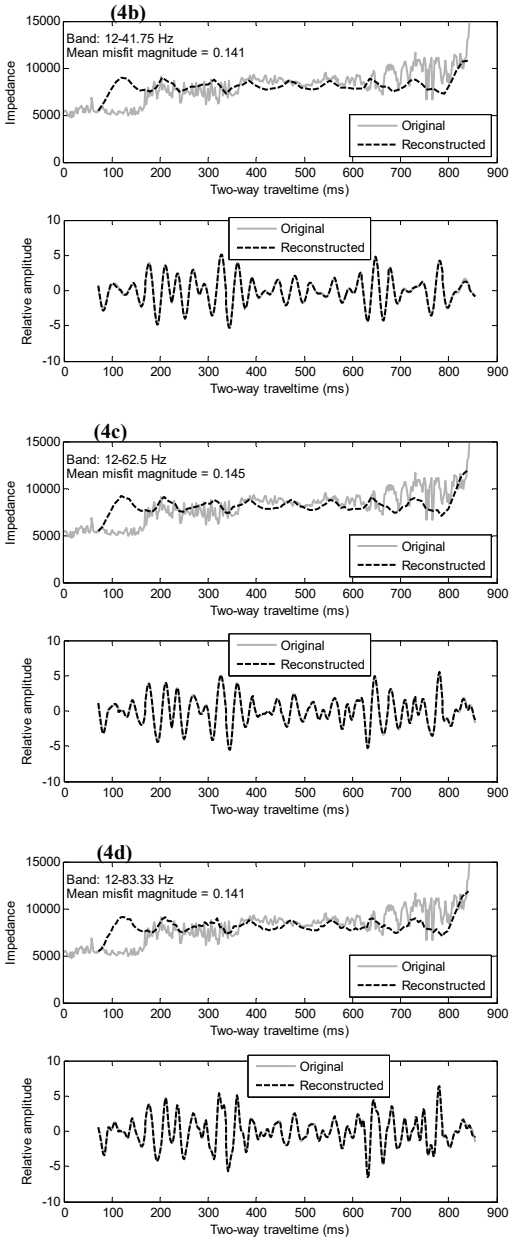

Figure 4: Comparison of original impedance with the reconstructed from field data (Figure 1c) (Upper panel); and Comparison of field data for corresponding frequency band with the data that the reconstructed models would give rise to (Lower panel). (a) 12–31.25 Hz, (b) 12–41.75 Hz, (c) 12–62.5 Hz, and (c) 12–83.33 Hz.

Discussion and Conclusions

Unlike the conventional approaches of impedance inversion, the present approach does not require a starting earth model or mathematical constraints on the earth reflectivity in order to overcome nonuniqueness (Veeken and Da Silva, 2004). Our approach provides a reliable solution to the existing problem of low-frequency impedance reconstruction from band-limited data. Nonuniqueness is countered in part by modeling the earth as a stack of homogeneous and horizontal layers and in part by the adoption of the SVD method for finding an optimal solution. The SVD method used here, rejects the smaller singular values, seeks a smooth solution, and recovers the cumulative reflection coefficients over sufficiently long time span, retaining the significant and relevant geologic information. In principle, the equation (2) can also be solved for the r_k's. However, it has been observed from our detailed trials that the resulting matrix equation for equation (2) will lead to singular values that do not have the range spanning as many orders of magnitude as available in the case of solving equation (5). Therefore, choices of discarding singular values will be fewer which will lead to poorer reconstruction than that of using equation (5). The assumption of impedance mean from a nearby well solves the problems (see subsection '*Tackling the reconstruction from field data*') of knowing the scale factor (between the true and relative seismic amplitude) and that of choosing the proper terminal singular value at onego.

Ghosh and Mandal (2016) has shown a way to reconstruct low-frequency part of the impedance profile from band-limited reflection data using first principles only and without requiring any initial model or mathematical constraints. They have demonstrated the efficacy of their approach with synthetic data. In this work, we have logically extended their work and proposed an approach for effective impedance reconstruction from field data. The successful reconstruction from field data also illustrate the internal consistency of the basic approach. The present work also establishes that the effective reconstruction of broad and smooth impedance profile is possible from first principles and band-limited field data. The major benefits of this low frequency impedance reconstruction are approximate estimation of impedance profile and its broad trend. These information can serve as reliable initial input for more refine inversion modeling or geologic interpretation.

References

Berteussen, K. A., and B. Ursin, 1983, Approximate computation of the acoustic impedance from seismic data: Geophysics, **48**, 1351–1358.

Ghosh, S. K., 2000, Limitations on impedance inversion of band-limited reflection data: Geophysics, **65**, 951–957. doi: 10.1190/1.1444791

Ghosh, S. K., and A. Mandal, 2016, Feasibility of approximate broadband estimation of acoustic impedance profile from first principles and band-limited reflection data: Geophysics, **81**(3), R57-R74. https://doi.org/10.1190/geo2015-0056.1

Oldenburg, D. W., T. Scheuer, and S. Levy, 1983, Recovery of the acoustic impedancefrom reflection seismograms: Geophysics, **48**, 1318–1337. doi: 10.1190/1.1441413

Press, W. H., B. P. Flannery, S. A. Teukolsky, and W. T. Vetterling, 1992, Numerical Recipes in C: The Art of Scientific Computing (Second ed.): Cambridge University Press.

Robinson, E. A., and S. Treitel, 1980, Geophysical signal analysis: Prentice-Hall, Inc.

Veeken, P. C. H., and M. Da Silva, 2004, Seismic Inversion Methods and some of their constraints: First Break, **22**, 47–70. doi: 10.3997/1365-2397.2004011